

lactose units) between the sheets, then the first few such insertions (three if the sheets are truly rigid) define the intersheet separation. Subsequent additions merely fill the available sites with no significant effect on the separation. Factors that will be sensitive to the number of filled sites in our case will be the ease of hydration, the tendency to form stiff gels by galactose-galactose complexation through suitable intermediates such as borate or heavy metals, and solubility. Recent  $^{13}\text{C}$  and  $^{11}\text{B}$  NMR also point to such interactions and suggest the particular involvement of galactose O3 and O4 from each of two different chains as the most likely complexation mode.<sup>22,23</sup> This same interaction is also implicit in the detailed modeling that is now in progress in our laboratory, and the structures of several galactomannans are being determined and refined by analysis of the X-ray intensity data.

**Acknowledgment.** We gratefully acknowledge partial support of this work by the donors of the Petroleum Research Fund, administered by the American Chemical Society, and Centre National de la Recherche Scientifique.

**Registry No.** Fenugreek gum, 73613-05-5; lucerne gum, 119618-90-5.

## References and Notes

- (1) Wintershall, A. G. Kalle & Co. A. G. Ger. Fe. Rep. Patent 1,017,560, 1957; *Chem. Abstr.* 1960, 54, 15921.

- (2) Githens, C. J.; Burnham, J. W. *Soc. Pet. Eng. J.* 1977, 5-10.
- (3) Rummo, C. W. *Oil Gas J.* 1982, 80, 84-89.
- (4) Swanson, B. L. U.S. Patent 4,425,241, 1984.
- (5) Bajaj, P.; Chaven, R. B.; Manjeet, B. *J. Macromol. Sci., Rev. Macromol. Chem. Phys.* 1984, C24, 387-417.
- (6) Wielinga, W. C. In *Gums and Stabilisers for the Food Industry 2*; Phillips, G. O., Wedlock, D. J., William, P. A., Eds.; Pergamon: Oxford, 1984; pp 251-276.
- (7) Reid, J. S. G.; Bewley, J. D. *Planta* 1979, 147, 145-150.
- (8) Uebelmann, G. Z. *Pflanzenphysiol.* 1978, 88, 235-53.
- (9) Dea, I. C. M.; Morrison, A. *Adv. Carbohydr. Chem. Biochem.* 1975, 31, 241-312.
- (10) Chien, Y. Y.; Winter, W. T. *Macromolecules* 1985, 18, 1357.
- (11) Bouckris, H.; Winter, W. T. *Macromolecules*, submitted.
- (12) Chanzy, H.; Pérez, S.; Miller, D. P.; Paradossi, G.; Winter, W. T. *Macromolecules* 1987, 20, 2407-2413.
- (13) Winter, W. T.; Bouckris, H.; Okuyama, K.; Arnott, S., unpublished results.
- (14) McCleary, B. V.; Neukom, H. *Prog. Food Nutr. Sci.* 1982, 6, 109-118.
- (15) McCleary, B. V. *Carbohydr. Res.* 1979, 71, 205-230.
- (16) Marchessault, R. H.; Buleon, A.; Deslandes, Y.; Goto, T. *J. Colloid Interface Sci.* 1979, 71, 375.
- (17) Sarko, A.; Muggli, R. *Macromolecules* 1974, 7, 486-494.
- (18) Gardner, K. H.; Blackwell, J. *Biopolymers* 1974, 13, 1975-2001.
- (19) Gardner, K. H.; Blackwell, J. *Biopolymers* 1975, 14, 1581-1595.
- (20) Atkins, E. D. T.; Hopper, E. D. A.; Isaac, D. H. *Carbohydr. Res.* 1973, 27, 29-37.
- (21) Nieduszynski, I. A.; Marchessault, R. H. M. *Can. J. Chem.* 1972, 50, 230-236.
- (22) Nobel, O.; Taravel, F. R. *Carbohydr. Res.* 1987, 166, 1-11.
- (23) Gey, C.; Nobel, O.; Pérez, S.; Taravel, F. R. *Carbohydr. Res.* 1987, 173, 175-184.

## Study on the Interconversion of Unit Structures in Polyaniline by X-ray Photoelectron Spectroscopy

T. Nakajima,\* M. Harada, R. Osawa, and T. Kawagoe

Technical Research Laboratory, Bridgestone Corporation, 3-1-1, Ogawahigashi-Cho, Kodaira-shi, Tokyo 187, Japan

Y. Furukawa† and I. Harada\*

Pharmaceutical Institute, Tohoku University, Aobayama, Sendai, 980, Japan.

Received June 28, 1988; Revised Manuscript Received November 28, 1988

**ABSTRACT:** XPS  $\text{N}_{1s}$  and valence spectra of various forms of polyaniline were studied and the compositions of four unit structures in some films were determined. A proposed scheme of interconversion of the unit structures by reduction/oxidation and acid/base treatment is useful to understand the interconversion mechanism of polyaniline. Reduced-base-treated polyaniline (1A, white) is taken as a standard material because it consists solely of imino-1,4-phenylene (IP) units ( $-\text{NHC}_6\text{H}_4-$ ). Electrochemical oxidation of 1A in nonaqueous medium converts part (46%) of IP into its radical cation ( $\text{IP}^{+\bullet}$ ) (doped 1A). Acid treatment of 1A changes some IP (28%) to its cation ( $\text{IP}^+$ ) (1S). Base treatment of doped 1A converts two  $\text{IP}^{+\bullet}$ -IP parts into two IP parts and one nitrilo-2,5-cyclohexadiene-1,4-diylidenenitrilo-1,4-phenylene (NP) ( $-\text{N}=\text{C}_6\text{H}_4=\text{N}-\text{C}_6\text{H}_4-$ ) part to give a sample which is practically the same as base-treated polyaniline (2A). Washing of as-polymerized polyaniline changes some  $\text{IP}^+$  to IP and some  $\text{IP}^{+\bullet}$  to NP (2S( $\text{H}_2\text{O}$ )). An earlier conclusion that the radical cation of imino-1,4-phenylene plays an important role in electrical conduction in polyaniline has been supported, and it is pointed out that a highly conducting form of polyaniline exhibits a finite density of state at the Fermi energy. A large change in the valence structure is also observed at 8.7 eV in polyaniline containing  $\text{IP}^{+\bullet}$ . The advantage of an electrochemical redox process in nonaqueous media over that in aqueous media for practical purposes is explained.

## Introduction

Polyaniline is an excellent material for electronic devices such as field-effect transistors,<sup>1</sup> electrochromic display,<sup>2</sup> solar battery,<sup>3</sup> etc. Actually it has been successfully applied to practical use as a rechargeable polymer lithium bat-

tery.<sup>4,5</sup> In order to improve such applied devices, it is important to elucidate the relation between polyaniline's structure and electrical property.

Polyaniline is known to take various forms via acid/base treatment and oxidation/reduction. In a preceding paper,<sup>6</sup> vibrational spectra of polyaniline were studied in detail and four unit structures in its various forms were identified. However, the composition in each form except the reduced-base-treated form (1A) has remained uncertain.

\* Present address: Department of Chemistry, Faculty of Science, The University of Tokyo, Bunkyo-ku, Tokyo 113, Japan.

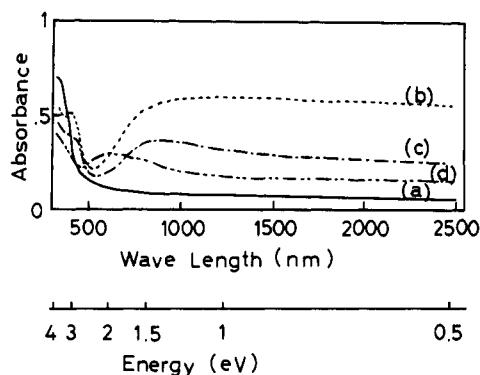


**Figure 1.** Visible-near-IR absorption spectra of (a) 1A, (b) doped 1A, (c) 1S, and (d) base-treated doped 1A (2A). For names of the polyaniline forms, see text.

We have utilized X-ray photoelectron spectroscopy (XPS) to evaluate the compositions in some of the polyaniline forms.

In the present paper, we report the XPS  $N_{1s}$  and valence spectra of 1A, acid-treated 1A (1S), doped 1A, base-treated doped 1A (2A), and water-washed polyaniline (2S( $H_2O$ )). Assignments of the spectra have been made referring to the data of *N,N'*-diphenyl-1,4-benzenediamine and its derivatives. The XPS  $N_{1s}$  peaks due to neutral ( $-NH-$  and  $-N=$ ), radical cationic ( $-NH^{+\bullet}-$ ), and cationic ( $-HN_2^+-$ ) nitrogens were observed separately and their compositions in doped 1A, 1S, and 2S( $H_2O$ ) have been determined. The two types of neutral nitrogen as well as the cation and radical cation gave characteristic peaks in the valence region, which were useful in studying the compositions in further detail. Interconversion schemes of the various forms are discussed in terms of those of unit structures.

## Experimental Section

**Low Molecular Weight Reference Compounds.** Colorless crystalline *N,N'*-diphenyl-1,4-benzenediamine,<sup>7</sup>  $C_6H_5NHC_6H_4NHC_6H_5$  (BBB, B denoting benzenoid), was a gift from Seiko Chemical Co., Ltd. *N,N'*-Diphenyl-1,4-benzenediamineditetrafluoroborate (BBB-2HBF<sub>4</sub>) was recrystallized from an aqueous ethanol solution. *N,N'*-2,5-Cyclohexadiene-1,4-diylidenebis(benzenamine),<sup>8</sup>  $C_6H_5N=C_6H_4=NC_6H_5$  (BQB, Q denoting quinoid), was synthesized by oxidation of BBB.<sup>9</sup> It was not possible to obtain an XPS sample of semiquinone radical cation of BBB (BBB<sup>•+</sup>),<sup>10</sup> because of its unstableness.<sup>11</sup>

**Water-Washed Polyaniline (2S( $H_2O$ )).** Polyaniline was obtained as a film by electrochemical oxidation of aniline in an aqueous solution of 2 M ( $M = \text{mol/dm}^3$ ) hydrofluoroboric acid and 1 M aniline on a 4-cm<sup>2</sup> platinum electrode under an electric current of 20 mA for 1.4 h. The film was washed with a large amount of distilled water for 10 h and dried under dynamic vacuum (2S( $H_2O$ )). The color was blue.

**Reduced-Base-Treated Polyaniline (1A).** 1A was prepared with a slight modification of the previous methods.<sup>6,12</sup> The film polymerized as described above was electrochemically reduced for 1 h in 1% hydrofluoroboric acid under an electric current of 4 mA. The resulting yellowish green film was immersed in 30% hydrazine aqueous solution for 24 h and the color became white. The film was washed in degassed methanol for 3 h and then dried under dynamic vacuum (1A). According to an elemental analysis, the atomic ratio was calculated to be  $C_{6.1}H_{5.1}N_{1.0}$  (C, 78.9 wt %; H, 5.5; N, 15.2; O, 0.4). The visible-near-IR spectrum of a thin film prepared on an ITO glass which is similar to that of BBB,<sup>13</sup> is shown in Figure 1a. The thin film was prepared by shortening the polymerization time to 10 s and by using hydrazine vapor instead of the aqueous hydrazine solution.

**Doped 1A.** The 1A film on the 4-cm<sup>2</sup> platinum electrode was electrochemically oxidized in propylene carbonate containing 1 M lithium tetrafluoroborate (electrolyte for a lithium battery, Mitsubishi Petrochemical Co., Ltd.). Aluminium-lithium alloy

(80 wt % Li, Foote Mineral Co.) was used as the counter electrode and 3.8 V was applied between the working and counter electrodes. Charged capacity was 140 Ah/kg (0.48 charge transfer per aniline unit). The resulting film was washed with degassed acetonitrile for 1 h and dried under dynamic vacuum (bluish green). The visible-near-IR spectrum in Figure 1b correlates with that of BBB<sup>•+</sup>,<sup>13</sup> namely, the absorption around 400 nm indicates the presence of radical cation. Recently, the direct evidence for the radical cation (IP<sup>•+</sup>) of doped 1A by EPR work was reported by Ohsawa et al.<sup>14</sup>

**Acid-Treated 1A (1S).** The 1A film was immersed in degassed aqueous solution containing 2 M hydrofluoroboric acid for 24 h and washed with degassed acetonitrile for 6 h. The resulting yellowish green sample was dried under dynamic vacuum. The visible-near-IR spectrum of a thin film is shown in Figure 1c.

**Base-Treated Doped 1A (2A).** Doped 1A film was immersed in aqueous solution of 1 M NaOH for 72 h and the color became blue. The resulting sample was washed with distilled water for 24 h and dried under dynamic vacuum. The atomic ratio was calculated from the data of elemental analysis,  $C_{6.2}H_{4.5}N_{1.0}$  (C, 78.7 wt %; H, 4.8; N, 14.9; F, 0.3; O, —). It was not possible to obtain the oxygen datum because of interference by fluorine. The visible-near-IR spectrum (Figure 1d) correlated with that of BQB.<sup>13</sup>

**X-ray Photoelectron Spectroscopy.** X-ray photoelectron spectra were recorded on a JEOL JPS-80 X-ray photoelectron spectrometer with unfiltered Mg K $\alpha$  (1253.6 eV) for spectra of both the core and the outer shell. With the voltage and the current of the X-ray tube higher than 15 kV and 25 mA, respectively, the samples were damaged as judged from the spectra. When the voltage and current were reduced to 10 kV and 15 mA, however, not much damage was noticed and the spectrum at the 40th scan was identical with the first scan. Measurements were performed under a vacuum of  $7 \times 10^{-7}$  Pa at room temperature. The binding energy of  $C_{1s}$  was adjusted to 284.6 eV, because it was identical in any form of polyaniline.<sup>15,16</sup> Prepared samples, which were rinsed in appropriate solvents as explained above, were kept in the vacuum desiccators separately in order to avoid possible contamination among them. A fresh surface of the sample was prepared by cutting with a surgical blade and the XPS spectrum was measured as soon as possible. The exposure to the atmosphere was less than 20 s. According to the survey scan spectra (0–1000 eV), no surface impurities but very slight traces of oxygen on the sample were found. Each  $N_{1s}$  spectrum was deconvoluted into Gaussian distributions, and the error between the summation of Gaussian deconvoluted area intensities and the observed area intensity remained less than 2%. Ion etching was not performed.

**Electrical Conductivity.** Electrical conductivity was measured on LORESTA-FP (Mitsubishi Petrochemical Co., Ltd.) with four probe electrodes in a drybox (Mecaplex Ltd.) filled with ultrahigh-quality argon (Toyo Sanso Co., Ltd.) at room temperature.

## Results

**Low Molecular Weight Reference Compounds.** The  $N_{1s}$  binding energy was 399.1 eV for the amine nitrogen ( $-NH-$ ) of BBB and 399.0 eV for the quinoid nitrogen ( $-N=$ ) of BQB. Accordingly, it is not possible to discriminate the two types of neutral nitrogens only from the  $N_{1s}$  spectra. The binding energy was 402.3 eV for cationic nitrogen ( $-NH_2^+$ ) in BBB-2HBF<sub>4</sub>. The measurement was not possible for the radical cation for the reason mentioned in the Experimental Section. One-to-one mixtures of BBB<sup>2+</sup>-BBB and BBB<sup>2+</sup>-BQB give  $N_{1s}$  spectra consisting of two peaks with area intensities (Gaussian deconvoluted) of 50% at 402.3 eV and 50% at 399.1 eV and 48% at 402.3 eV and 52% at 399.0 eV, respectively. This result signifies that the area intensities per nitrogen are practically the same for the three species, IP, IP<sup>+</sup>, and NP, at least in the model compound. In the XPS valence spectrum of BBB, four peaks appeared at 17.5, 14.1, 11.7, and 9.6 eV. On the basis of the assignments for aniline,<sup>17</sup> they are assigned as follows: 17.5 eV, one or an overlap of  $e_{2g}$ ,  $a_{1g}$ ,  $b_{1u}$ , and  $b_{2u}(NH)$ ; 14.1 eV, one or an overlap of  $e_{1u}$ ,  $a_{2u}$ , and  $b_{2u}(NH)$ ;

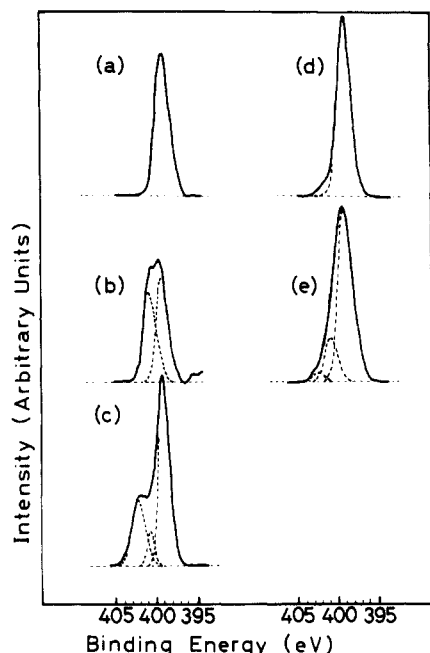


**Figure 2.** XPS,  $N_{1s}$  spectra of (a) 1A, (b) doped 1A, (c) 1S, (d) base-treated doped 1A (2A), and (e) water-washed polyaniline ( $2S(H_2O)$ ). Dotted lines are the result of Gaussian deconvolution.

11.7 eV,  $LP_N$  (one of the lone pair electrons of N) and  $e_{2g}$ ; 9.6 eV,  $e_{1g}$ . The spectrum of BQB with peaks at 18.0, 14.3, 9.5, 3.0, and 1.5 eV is different from that of BBB especially in the 3.0–1.5-eV region. The peaks at 18.0, 14.3, and 9.5 eV arise from the two benzenoid rings at both ends. The 11.7-eV peak in BBB is missing in BQB because it has a contribution from the lone pair of  $-NH-$  which is converted to  $-N=$  in BQB. The 3.0- and 1.5-eV peaks are characteristic of a conjugated structure of double and single bonds.<sup>18</sup> The spectral pattern of BBB- $2HBF_4$  is similar to that of BBB: 17.5, 14.0, 10.5, and 9.4 eV, in which the deviation of the third peak from that in BBB is noticeable. This is due to the lack of lone pair electrons in this species.

**Reduced-Base-Treated Polyaniline (1A).** In the XPS  $N_{1s}$  spectrum of white 1A (Figure 2a), a single narrow peak was observed at 399.1 eV which is close to those of BBB and BQB. The result of elemental analysis indicates that 1A consists solely of  $NHC_6H_4$  units. Vibrational analysis has shown that the units are linked at para positions.<sup>6</sup> Accordingly, the peak is assigned to the nitrogen in the imino-1,4-phenylene unit (IP). The XPS valence spectrum (Figure 3a) consists of two major peaks at 17.5 and 14.0 eV and two minor peaks at 11.0 and 9.0 eV. The pattern corresponds well with that of BBB. Electrical conductivity of this film was lower than  $10^{-5} S cm^{-1}$ .

**Doped 1A Polyaniline.** Two  $N_{1s}$  peaks were observed at 399.1 and 400.8 eV (Figure 2b). These peaks are assigned to IP and its radical cation ( $IP^{+}$ ), respectively, based on the results of visible and vibrational spectroscopy.<sup>6</sup> The Gaussian deconvolution (dotted line) suggests 46%  $IP^{+}$  and 54% IP in the sample on the assumption that the area intensities are proportional to the compositions. This assumption is supported by the observation that the area intensity of the band on the high binding energy side in the spectra of doped 1A at various doping levels was proportional to the amount of the dopant anion.<sup>19</sup> This composition corresponds well with the electrochemical doping level (0.48). The XPS valence spectrum (Figure 3b) is dominated by a very strong peak at 8.7 eV, presumably due to  $IP^{+}$ . The peaks due to  $\pi$ -electrons in the benzenoid ring observed in 1A and 1S (see below) are absent, indicating that the energy levels in the

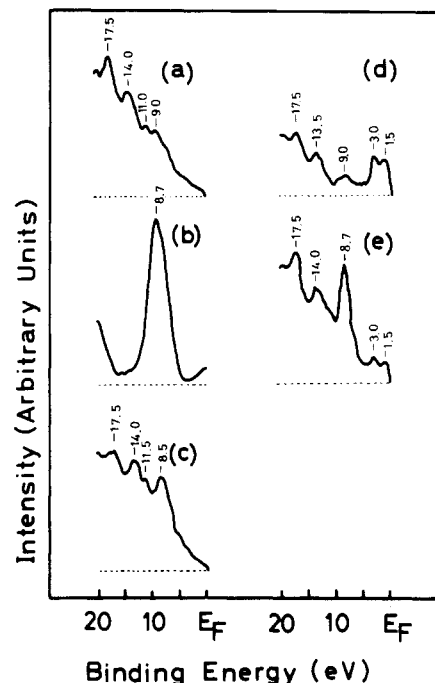


**Figure 3.** XPS valence spectra of (a) 1A, (b) doped 1A, (c) 1S, (d) base-treated doped 1A (2A), and (e) water-washed polyaniline ( $2S(H_2O)$ ). The peak in (b) was estimated to be more than four times stronger than the strongest peak in (a), (c), and (d).

benzenoid ring in IP are greatly perturbed by enhanced interaction with an unpaired electron on N in  $IP^{+}$ . The 8.7-eV peak is so deep from Fermi energy that it cannot play a role in electrical conduction, but it is a useful key peak of  $IP^{+}$ . An increase in electron density is observed toward  $E_F$ , indicating that Fermi energy is located in the conduction band, which may be related to the high electrical conductivity ( $>5 S cm^{-1}$ ).<sup>18</sup> According to previous works,<sup>15,16</sup> such phenomenon as an increase in electron density toward  $E_F$  had not been observed; only some weak signal at  $E_F$  was reported.<sup>15</sup>

**Acid-Treated Polyaniline 1A (1S).** The XPS spectrum (Figure 2c) can be deconvoluted into three Gaussian peaks (dotted line in Figure 2c) at 402.4, 400.8, and 399.1 eV. The 402.4-eV peak is assigned to  $N^{+}$  in the positive salt unit of IP ( $IP^{+}$ ) by referring to the binding energy of BBB- $2HBF_4$ . The 399.1-eV peak arises from IP on the basis of the vibrational spectra which shows that 1S consists mostly of IP and  $IP^{+}$ .<sup>6</sup> A weak peak at 400.8 eV is assigned to radical cation (mentioned above). Some residual oxidizing agents such as oxygen contaminated in the acid solution would have generated this species. The presence of radical cation is also indicated in the 400-nm region of the absorption spectrum (Figure 1c). The compositions of three species in this particular sample are IP, 64%;  $IP^{+}$ , 28%; and  $IP^{+}$ , 8%. Among the four peaks in the valence spectrum (Figure 3c), those at 17.5, 14.0, and 11.5 eV are assigned to overlaps of the peaks arising from IP and  $IP^{+}$ . The peak at 8.5 eV is possibly assigned to the minor component  $IP^{+}$ . Electrical conductivity was lower than  $10^{-5} S cm^{-1}$ .

**Base-Treated Doped 1A (2A).** According to elemental analysis, base-treated doped 1A has the same composition as that of 2A,<sup>20</sup> and actually it was proved that it consists of IP and nitrilo-2,5-cyclohexadiene-1,4-diylidenenitrilo-1,4-diylidenenitrilo-1,4-phenylene (NP) units ( $-N=C_6H_4=N-C_6H_4-$ ) by vibrational spectroscopy.<sup>6</sup> The  $N_{1s}$  peak (Figure 2d) at 399.1 eV is similar to that of 1A (Figure 2a) except for a weak shoulder on the higher energy side in the former. The main peak in Figure 2d is assigned to

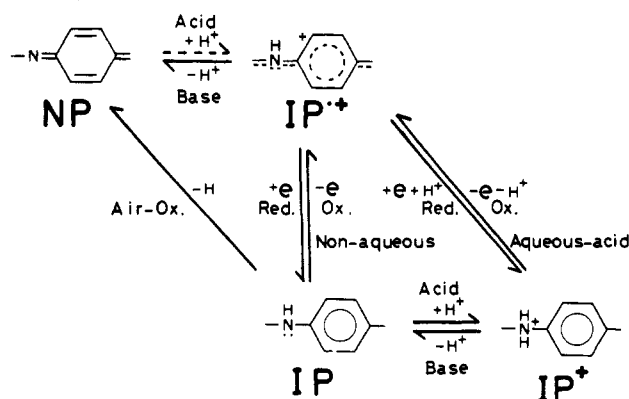


Figure 4. Scheme of interconversion of four unit structures.

an overlap of IP and NP, which lie at practically the same binding energy. The shoulder is assigned to residual  $IP^{+\bullet}$ . In contrast to the  $N_{1s}$  region, the valence spectrum (Figure 3d) is much different from that of 1A (Figure 3a). It is reasonably explained as a mixture of those of IP and quinone diimine structures. It should be noted that the electron density has zero value at Fermi energy. Electrical conductivity is less than  $10^{-6} \text{ S cm}^{-1}$ , which is lower than that of 1A, which implies that the electron conducting capability of quinone diimine is less than that of IP.

**Water-Washed Polyaniline (2S( $H_2O$ )).** The  $N_{1s}$  peaks with a shoulder on the higher binding energy side were deconvoluted (Figure 2e) and the compositions are  $IP^{+\bullet}$ , 4%;  $IP^{+\bullet}$ , 17%; and IP and/or NP, 79%. The XPS valence spectrum (Figure 3e) is explained as an overlap of those of IP (17.5 and 14.0 eV), NP (3.0 and 1.5 eV), and  $IP^{+\bullet}$  (8.7 eV). Judging from the intensities of the IP and NP peaks, the relative content of NP versus IP is smaller than that in 2A. Electrical conductivity was about  $0.3 \times 10^{-2} \text{ S cm}^{-1}$ .

## Discussion

The present XPS results are consistent with those found by elemental analysis and visible and vibrational spectroscopy,<sup>6,21</sup> that polyaniline takes four unit structures, IP,  $IP^{+\bullet}$ ,  $IP^+$ , and NP. In addition, the compositions in some films have been obtained, which is useful to elucidate the mechanism of interconversion of four structures and the related change in electrical conductivity.

When 1A, which consists solely of IP, was electrochemically oxidized (doped) in nonaqueous medium, 46% of the IP parts were converted to  $IP^{+\bullet}$ . Acid treatment of 1A converts part of IP into  $IP^+$  (28%) (1S). The small amount (8%) of  $IP^{+\bullet}$  found in 1S indicates that oxidation also proceeded to some extent. Previously, it was found that a consecutive IP-IP is oxidized by gaseous oxygen to give an NP.<sup>6</sup> Accordingly, IP can be converted into  $IP^{+\bullet}$  by electrochemical oxidation in nonaqueous medium,  $IP^+$  by acid treatment, and NP by oxygen treatment (Figure 4). The reverse reactions are possible except for the last one, which has not been tested (Figure 4). 2A can be obtained by base treatment of 2S or doped 1A. The XPS  $N_{1s}$  peak was very similar to that of 1A, while the valence spectrum was explained by those of IP and NP. As mentioned in a previous paper,<sup>6</sup> two  $IP^{+\bullet}$ -IP in 2S can be converted to an NP and an IP-IP by a disproportionation reaction. This reaction is shown in an abbreviated way at the top of Figure 4. Reversal of NP to  $IP^{+\bullet}$  may not be so efficient even in acid medium, because the reported intensity of the 8.7-eV XPS peak of acid-treated 2A<sup>15</sup> relative to that of the 17.5-eV peak seems to be lower than that of doped 1A in Figure 3b, where the 17.5-eV peak is hardly detectable on that scale. Definitely, conversion of NP into  $IP^{+\bullet}$  is not

possible in nonaqueous medium because of the lack of protons in the system. An electrochemical redox process in aqueous medium between  $IP^{+\bullet}$  and  $IP^+$  has been verified by in situ interconversion of the Raman spectra<sup>21</sup> (Figure 4).

The high conductivity of polyaniline-doped 1A is ascribable to  $IP^{+\bullet}$ , because the doped 1A film consists of only IP and  $IP^{+\bullet}$  and the conductivity of consecutive IP parts must be low ( $10^{-6} \text{ S cm}^{-1}$  in 1A). This is supported by the observation that doped 1A exhibits a finite density of state at the Fermi energy, while 1A does not (Figure 3). As mentioned above, the XPS valence spectrum of doped 1A indicates delocalization of electrons of the benzene ring and nitrogen. Such electron delocalization seems to be essential to the high electrical conductivity.

The conductivity of 2S( $H_2O$ ),  $0.3 \times 10^{-2} \text{ S cm}^{-1}$ , is much lower than that of 2S reported earlier ( $2.6 \text{ S cm}^{-1}$ ).<sup>6</sup> This is because the amount of  $IP^{+\bullet}$  was diminished by the heavy washing with water. If washed with distilled water of neutral pH,  $IP^+$  is efficiently converted into IP but  $IP^{+\bullet}$  also tends to be converted to NP (Figure 3e). As the result, the amounts  $IP^+$  and  $IP^{+\bullet}$  in 2S( $H_2O$ ) are much less than those in less washed 2S as is evident from the  $N_{1s}$  band analysis. As mentioned above, the amount of NP formed by this treatment is much less than that in 2A obtained by base treatment of doped 1A (Figure 3d,e).

White polyaniline 1A has been obtained by reduction of as-polymerized polyaniline (2S) in acid medium followed by hydrazine treatment. By this method  $IP^{+\bullet}$  in 2S is reduced to  $IP^+$  in the first step and all the  $IP^+$  parts are converted to IP in the second step. The use of hydrazine in the second step is important to obtain white polyaniline. It keeps the medium reducing during the base treatment. In an oxidizing base environment, IP converted from  $IP^+$  by base treatment is further changed first to  $IP^{+\bullet}$  (by oxidation) and then immediately to NP (by base treatment) and the color turns blue. Accordingly, in order to obtain white 1A it is necessary first to reduce  $IP^{+\bullet}$  into  $IP^+$  and second to convert  $IP^+$  into IP in a reducing environment.

Electrochemical redox interconversion of  $IP^{+\bullet}$  and IP in nonaqueous medium has been applied to a rechargeable lithium battery.<sup>4,5</sup> The presence of NP in the system is useless because it cannot contribute to the discharge process but reduces the doping level to diminish the capacity. NP is changed into  $IP^{+\bullet}$  in a proton donative environment, such as aqueous acid solution, but the process is not very efficient. Hence, the discharge capacity of polyaniline in aqueous acidic electrolyte is less than that in nonaqueous electrolyte which stabilizes  $IP^{+\bullet}$ .

## Conclusion

A combined study of XPS  $N_{1s}$  and valence spectra of various forms of polyaniline has made it possible to estimate the compositions of four unit structures contained in them. White polyaniline 1A is a pure  $(1,4\text{-NHC}_6\text{H}_4)_n$  ( $(IP)_n$ ). Electrochemical oxidation of 1A converts 46% of IP into its radical cation ( $IP^{+\bullet}$ ). About 28% of IP is changed to cation ( $IP^+$ ) by acid treatment of 1A and some  $IP^{+\bullet}$  is formed. Two  $IP^{+\bullet}$ -IP parts in doped 1A are neutralized by base treatment to give two IP parts and an  $\text{—N=C}_6\text{H}_4\text{=N—C}_6\text{H}_4\text{—}$  (NP) part by disproportionation. Washing of as-polymerized polyaniline with water changes some  $IP^+$  to IP and some  $IP^{+\bullet}$  to NP. These interconversions of various forms are consistently explained by an interconversion scheme of the four unit structures. Among the four structures, radical cation of imino-1,4-phenylene plays an important role in the electrical conduction because it exhibits a finite density of state at the Fermi energy.

The advantage of the electrochemical redox process between IP and IP<sup>•+</sup> in nonaqueous medium over that in aqueous medium for practical purpose is reasonably understood.

**Registry No.** BBB, 74-31-7; BBB-2HBF<sub>4</sub>, 119393-41-8; BQB, 6246-98-6; lithium tetrafluoroborate, 14283-07-9; polyaniline, 25233-30-1.

## References and Notes

- (1) Paul, E. W.; Ricco, A. J.; Wrighton, M. S. *J. Phys. Chem.* **1985**, *89*, 1441.
- (2) Kitani, A.; Yano, J.; Sasaki, K. *J. Electroanal. Chem.* **1986**, *209*, 227.
- (3) Kaneko, M.; Nakamura, H. *J. Chem. Soc., Chem. Commun.* **1985**, 346.
- (4) Enomoto, T.; Allen, D. P. *Bridgestone News Release* **1987**, Sept 9. Address of T. Enomoto: International Public Relations, Bridgestone Corporation, 1-10-1, Kyobashi, Chuo-ku, Tokyo 104, Japan.
- (5) *Chem. Week* **1987**, Oct 14, 40.
- (6) Furukawa, Y.; Ueda, F.; Hyodo, Y.; Harada, I.; Nakajima, T.; Kawagoe, T. *Macromolecules* **1988**, *21*, 1297.
- (7) This compound is also called *N,N'*-diphenyl-*p*-phenylenediamine (DPPD) and *N,N'*-diphenyl-*p*-benzoquinone diamine (QDA).
- (8) This compound is also called *N,N'*-diphenyl-*p*-quinone diimine (DPQI) and *N,N'*-diphenyl-*p*-benzoquinone diimine (QDI).
- (9) Honzl, J.; Metalová, M. *Tetrahedron* **1969**, *25*, 3641.
- (10) Linschitz, H.; Rennert, J.; Korn, T. M. *J. Am. Chem. Soc.* **1954**, *76*, 5839.
- (11) Hagiwara, T.; Demura, T.; Iwata, K. *Synth. Met.* **1987**, *18*, 317.
- (12) Nakajima, T.; Toyosawa, S.; Suzuki, K.; Miyazaki, T.; Kitamura, T.; Kawagoe, T. Japan Patent Pub. 62-149724, 1987.
- (13) Linschitz, H.; Ottolenghi, M.; Bensasson, R. *J. Am. Chem. Soc.* **1967**, *89*, 4592.
- (14) Ohsawa, T.; Kabata, O.; Kimura, O.; Yoshino, K. reported in the International Conference on Science and Technology of Synthetic Metals, June 26-July 2, 1988, Santa Fe and: *Synth. Met.*, in press.
- (15) Salaneck, W. R.; Lundström, I.; Hjertberg, T.; Duke, C. B.; Conwell, E.; Paton, A.; MacDiarmid, A. G.; Somasiri, N. L. D.; Huang, W. S.; Richter, A. F. *Synth. Met.* **1987**, *18*, 291.
- (16) Snauwaert, P.; Lazzaroni, R.; Riga, J.; Verbist, J. J. *Synth. Met.* **1987**, *18*, 335.
- (17) Palmer, M. H.; Moyes, W.; Spiers, M.; Ridyard, J. N. A. *J. Mol. Struct.* **1979**, *53*, 235.
- (18) Stafström, S.; Brédas, J. L.; Epstein, A. J.; Woo, H. S.; Tanner, D. B.; Huang, W. S.; MacDiarmid, A. G. *Phys. Rev. Lett.* **1987**, *59*, 1464.
- (19) Okabayashi, K.; Hyodo, S. *Proceedings of the 54th Spring Meeting of the Chemical Society of Japan*; Tokyo, 1987; p 124.
- (20) MacDiarmid, A. G.; Chiang, J. C.; Richter, A. F.; Epstein, A. J. *Synth. Met.* **1987**, *18*, 285.
- (21) Furukawa, Y.; Hara, T.; Hyodo, Y.; Harada, I. *Synth. Met.* **1986**, *16*, 189.

## Investigation of Diffusion in Polystyrene Using Secondary Ion Mass Spectroscopy

S. J. Whitlow and R. P. Wool\*

*Department of Materials Science and Engineering, University of Illinois, 1304 W. Green Street, Urbana, Illinois 61801. Received August 8, 1988; Revised Manuscript Received November 22, 1988*

**ABSTRACT:** SIMS is an ideal tool for examining polymer diffusion because it combines excellent depth resolution with direct depth profile measurement. This is a preliminary study on the use of SIMS for measuring depth profiles of polymers. Bilayer samples composed of  $\bar{M}_w = 111\,000/93\,000$  deuterated-protonated monodisperse polystyrene films were chosen for this investigation. The deuterated film was  $\approx 1000$  Å thick and the protonated film was  $\approx 2500$  Å thick. Before testing, samples were covered with 200 Å of Au to prevent charging. Analysis of a sharp interface showed a depth resolution of 138 Å, significantly better than that of several other methods. The depth profile was measured for a bilayer after annealing at 125 °C for 14 400 s. The diffused profile was analyzed by using the Grube method and the self-diffusion coefficient,  $\bar{D}$ , was found to be  $5.6 \times 10^{-16}$  cm<sup>2</sup>/s.

## Introduction

Understanding polymer diffusion is important for controlling mechanical properties of melt-processed polymer blends and welded polymers. Recent techniques used to study polymer melt diffusion include forward recoil spectroscopy<sup>1,2</sup> (FRES), IR spectroscopy,<sup>3,4</sup> photobleaching,<sup>5</sup> and small-angle neutron scattering (SANS).<sup>6,7</sup> This paper presents a new approach for measuring polymer diffusion, namely, the application of secondary ion mass spectroscopy (SIMS). Like the above methods, SIMS is sensitive to both hydrogen and deuterium which makes it useful for tracer studies. The primary advantages of SIMS are that it has excellent depth resolution and it is able to directly measure a concentration profile. Also, this technique can monitor elements to much greater depths than some of the above methods.

SIMS has long been an important tool for the analysis of semiconductors but little work has been done on polymers. Most SIMS applications used the static (low-energy

primary beam) mode to characterize polymer surfaces by their mass spectra.<sup>8,9</sup> Relatively little work has been done on depth profiling of polymers<sup>10,11</sup> with no quantitative analysis. This paper will present a quantitative analysis of diffusion in a deuterated-protonated polystyrene bilayer system.

## SIMS

The basis for SIMS is the ejection of charged atoms and molecules caused by an impinging ion beam. The incoming primary ion transfers energy and momentum to the region around the point of impact. One result of this event is loss of surface material by sputtering.<sup>12</sup> A second result is changes in the target structure known as atomic mixing.<sup>13</sup>

The sputtering process is shown schematically in Figure 1. The incoming primary ion dissipates a large portion of its energy in the region near the surface. The average distance a primary ion penetrates the sample is known as the primary ion range. This parameter characterizes the